

# Highly Sensitive Photonic Sensor Based on V-Shaped Channel Mediated Gold Nanowire

M. Omri, F. Ouerghi, F. AbdelMalek and S. Haxha, Senior Member, *IEEE*

**Abstract**— This paper presents a highly sensitive Surface Plasmon Resonance (SPR) biosensor using gold (Au) nanowires mediated single and double V-Shaped Channels (VSC). The proposed sensor consists of an Au nanowire placed under the VSC region, which is coupled to the light source. The sensing process is performed through the mediation of the SPR between the surface plasmon polaritons and the core guided modes of the VSC, which is later filled with analytes to be measured. The sharp edge of the VSC enhances the concentration of the magnetic fields allowing the detection of small changes in the refractive index of the analytes (biomolecules). Due to the important optical properties of the nanowire in nanoscale confinement, the inner and outer radii are optimized to obtain high sensitivity. The sensitivity is calculated to be 9230 nm/Refractive Index Unit (RIU) for a single VSC, while it is greatly enhanced reaching 15384 nm/RIU for double VSC system. The double V channels have distinctive responses to different analytes, which enables simultaneous sensing of various biomolecules. These excellent properties of the proposed Proof of Concept (PoC) photonic sensor pave the way to design multichannel compact sensors for a wide range of applications varying from chemical to biological sensing and detecting the cellular origin of infectious disease.

*Index Terms*—High sensitivity, Nanosensor, Double V-shaped channel, gold- nanowire, Surface Plasmon

## I. INTRODUCTION

Surface Plasmon Resonance (SPR) sensors are optical devices that are based on guided electromagnetic waves that propagate along a metal and dielectric interface. In both mediums the light propagation decays exponentially, and the detection process occurs due to the resonant coupling between the conduction electrons and the out medium. The SPR sensors have attracted increasing interest and have been under intensive study [1, 2] due to their high performance in terms of miniaturization, able to overcome diffraction limits, fast reaction and high sensitive to small refractive index changes [3, 4]. The coupling between the sensing region and the medium (analyte under test) results in changes in the effective refractive index. This change leads to a shift in resonance wavelength, thus the measurement of the sensitivity can be performed.

Various SPR sensor have been proposed to measure the refractive index changes, such as Bragg gratings [5], a slit waveguide coupled with a nanodisk resonator [6], photonic crystal fiber with a concave shape [7], also the study of

radiation effect on nanocrystalline TiO<sub>2</sub> layer has been reported in Ref. [8], ring resonators [9-10], a hexagonal cavity [11]. M. Li *et al* have demonstrated SPR refractive index sensor by using combination of plasmonic waveguide and nanocavity to detect changes in the refractive index with high sensitivity of 1000-2000 nm per refractive index unit (RIU) [12]. In [13], a plasmonic silicon waveguide for gas detection with sensitivity of 458 nm/RIU has been demonstrated, also L. Zhou *et al.*, have also presented miniaturized microring resonator sensor using hybrid plasmonic waveguide with sensitivity of 580 nm/RIU [14]. Additionally, a biosensor based on metal-insulator-silicon waveguide has been theoretically investigated with the sensitivity of 430 nm/RIU [15]. Nagiyalo *et al.* have demonstrated fiber-tip plasmonic resonators for label-free detection [16]. Further, an ellipsoidal Al nanoshell based sensor with spectral sensitivity of 4111.4 nm/RIU and minimum detectable refractive index of  $2.45 \times 10^{-5}$  RIU was reported [17]. A hybrid-plasmonic mode sensor with the sensitivity of about 1080 nm/RIU has been theoretically investigated to detect the refractive index changes [18]. Various kinds of SPR sensors based on photonic crystal fibers with excellent properties have been investigated and reported [19]. A microfluidic channel sensor based on a single mode fiber with large D shaped with a sensitivity of 11000 RIU/nm has been proposed in ref [20]. These optical sensors based on photonic crystal fibers suffer from many drawbacks such as bulky size and complex structures, from last decade. There has been great attempt to design, miniaturize and adapt traditional bulky structures and increase the SPR optical sensors sensitivity. Due to SPRs, the light can be confined to the surface of the metal where the surface waves interact strongly with the analyte in the sensing region. Among all metallic elements, gold (Au) and silver (Ag) are the most useful elements in sensing applications due of their low damping constant and they have high electronic conductivity. Gold compared to silver has better chemical stability in presence of

This project was funded by the Deanship of Scientific Research (DSR), King Abdulaziz University, Jeddah, under grant No. (D-294-305-1441). The authors, therefore, gratefully acknowledge the DSR technical and financial support.

M.Omri is with Deanship of Scientific Research, King Abdulaziz University, Jeddah, Saudi Arabia., (e-mail: omrimoha2002@yahoo.fr).

F. Ouerghi is with Faculty of Sciences, Jeddah University, Jeddah, Saudi Arabia, and National Institute of Engineers, University of Carthage, Tunis, Tunisia. (email: ouerghi.fauzi@gmail.com).

F. AbdelMalek is with National Institute for Applied Science and Technology, PB 676, Cedex 1080, University of Carthage, Tunis, Tunisia, and Faculty of Sciences, Jeddah University, Jeddah, Saudi Arabia. (email: fathi.amalek@gmail.com).

S. Haxha is Head of Microwave Photonics and Sensors, with Department of Electronic Engineering, School of Engineering, Physical and Mathematical Sciences, Royal Holloway, University of London, Egham, Surrey, TW20 0EX, United Kingdom. (email: [Shygyri.Haxha@rhul.ac.uk](mailto:Shygyri.Haxha@rhul.ac.uk)).

water, also at nanoscale size, it has attractive feature for next generation plasmonics based sensors.

The V-shaped channel structure proposed in this research work has advantages in terms of light confinement, especially in its bottom section, so that the light interacts strongly with the analytes placed in the VSC sensing region. In addition, this structure exhibits a strong localization of fields which can be used to improve the sensitivity and the selectivity of the sensor.

In this paper, we report a design of compact SPR refractive index sensor with gold coated on the surface of the external radius of the nanowire. The gold nanowire is deposited on the bottom section of the VSC region, which can be coupled to the bus waveguide. Around the nanowire, the plasmonic modes take place [21] where they couple with core guided modes at a particular wavelength, and the resonance mode get excited resulting in a resonance peak. At the resonance wavelength, the light is strongly coupled to the VSC region where a peak in transmission spectra takes place. In sensing medium, the resonance wavelength shifts due to the light-analyte interaction therefore, the resonance wavelength ( $\lambda_{res}$ ) can be detected by photodetectors at the output port of the proposed structure.

Using the Au nanowire mediated VSC sensing region makes the proposed structure more compact and simpler to fabricate with high sensitivity. By adjusting structural parameters such as the radius of Au nanowire and the gaps between the V-shape and light source, the performances of the sensor is greatly enhanced.

## II. DESIGN AND PRINCIPLES OF THE PLASMONIC BIOSENSOR

The proposed sensor structure is illustrated in Fig.1. The sensor design consists of a bus waveguide where a source is placed in the input section, above the silicon dioxide layer, which is etched to form the V-shaped channel-based sensing region. The proposed design is integrated on Si substrate. Gold nanowire is deposited between the bus waveguide and sensing medium to mediate the energy transport. The inner radius  $r_{in}$  is 465nm and the outer radius  $r_{out}$  is 589 nm, the refractive indices of silicon dioxide and silicon are 1.45 and 3.24, respectively. The in house Finite Difference Time Domain (FDTD) method with a perfectly matched layer (PML) as the boundary condition [22] is employed to investigate, analyze and optimize the transmission and sensing properties of the proposed structure. The FDTD requires a fine mesh and accurate time calculations as;

$$\Delta t = \frac{1}{c \sqrt{\frac{1}{\Delta x^2} + \frac{1}{\Delta z^2}}} \quad (1)$$

Where  $c$  is the speed of light in the free space and the meshing size is  $\Delta z = \Delta x = a/16$ , where  $a$  is the lattice constant, which is equal to 310 nm.

The gold nanowire has a relative permittivity given by Drude-Lorentz model [23]. The Drude-Lorentz model provides more

accurate prediction of permittivity and take into account the electronic transitions in gold.

$$\epsilon_{DL} = \epsilon_{\infty} - \frac{\omega_D^2}{\omega(\omega + j\gamma_D)} - \frac{\Delta\epsilon \times \Omega_L^2}{(\omega^2 - \Omega_L^2) + j\omega\Gamma_L} \quad (2)$$

Where the high frequency dielectric constant is  $\epsilon_{\infty} = 5.967$ , the weighted coefficient  $\Delta\epsilon = 1.09$ . Also,  $\omega$  stands for the guiding optical angular frequency,  $\omega_D$  is the plasmon frequency,  $\gamma_D$  is the damping frequency,  $\Omega_L$  represents the oscillator strength of the Lorentz oscillator, and  $\Gamma_L$  is the frequency spectrum width of the Lorentz oscillator. The proposed sensor, illustrated in Fig. 1, has major benefits in terms of integration, sensitivity, compactness and light confinement.

## III. RESULT AND DISCUSSIONS

The working principle of the proposed SPR sensor is based on the interaction of the evanescent field of the propagating light with the plasma of gold nanowire, which produces surface plasmon waves. The SPR occurs under certain conditions, among these conditions is when the electromagnetic field matches the frequency of free electron on the Au surface, consequently, strong and sharp resonances arise. When the incident light (a Transverse Magnetic (TM)) field placed at the input of the bus waveguide reaches the Au nanowire, the incident photons gain momentum and then excite the Surface Plasmon Polaritons (SPPs) at certain wavelength. The wavevector of the SPP can be expressed [24];

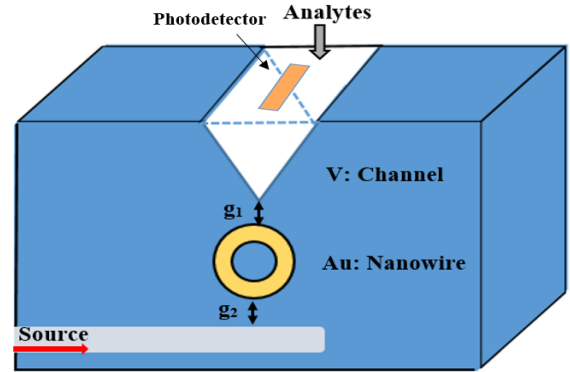


Fig. 1. Three-dimensional view of the proposed structure, the source is placed in the bus waveguide, the gold Au nanowire assisted the V-sensing region. The separation distance  $g_2$  couples light into the nanowire, while  $g_1$  plays a crucial role in transmitting the coming light to the analytes to be detected.

$$K_{spp} = \frac{\omega}{c} \left( \frac{\epsilon_d \epsilon_{Au}}{\epsilon_d + \epsilon_{Au}} \right)^{1/2} \quad (3)$$

where,  $\omega$  is the angular frequency in free-space,  $c$  is the speed,  $\epsilon_{Au}$  and  $\epsilon_d$  are the relative permittivities of Au and the dielectric, respectively.

The operation principle of the proposed sensor is based on the

light interaction, at resonance, when the maximum light is transmitted and transferred from the Au nanowire into the VSC region where the analytes are placed.

At the sharp edge of the VSC region, the  $H$ -field is highly confined, enabling the detection of small changes in the sensing medium. This change leads to a shift in the frequency response, by investigating the amount of the shift, the sensitivity can be systematically determined. Most of sensors have to be evaluated with respect to their sensitivity, which is related to the strength of the light and analyte interactions. In this regard, we concentrated to enhance the confinement of light in the sensing region, in order to achieve, the FDTD method is used to calculate and determine the electric field distribution in the V-region. The effect of the nanowire radii on the resonance wavelength and therefore on the sensitivity is of great importance. In order to obtain high sensitivity of the proposed sensor, we vary the inner and outer radii of the nanowire along with the separation distances  $g_1$  and  $g_2$ . In the beginning, we study the effect of the thickness  $\Delta r = r_{out} - r_{in}$  of the nanowire on the resonance peaks. By setting  $g_1$  and  $g_2$  to 31 nm, and varying the radii in such way that  $\Delta r = 7$  nm, the plots of  $H_x$  field for SPP mode along the  $x$ -axis at the bottom edge of the VSC region is depicted in Fig. 2. It should be stated that the near-field plots are calculated at  $\lambda = 1.55 \mu\text{m}$ . From this figure, it can be observed that the  $H_x$  field pattern is localized in the V-region, while its intensity is not well confined. Consequently, there is a tradeoff between the confinement and the light intensity. We further increase  $\Delta r$  from 7 nm to 10 nm, while  $g_1$  and  $g_2$  are kept equal to 31 nm, the corresponding  $H_x$  field distribution plot is depicted in Fig. 3.

Next, we vary the separation distance as  $g_1 = 29$  nm and  $g_2 = 33$  nm, while  $\Delta r$  is set to 10 nm. The  $H_x$  field pattern results are shown in Fig.4 where it can be clearly seen that light intensity is weakly confined in the VSC region due to the increase of the loss caused by increasing the  $g_2$  distance. We kept optimizing these key structure parameter where by decreasing the  $g_2$  from 33 nm to 29 nm, the  $H_x$  field pattern

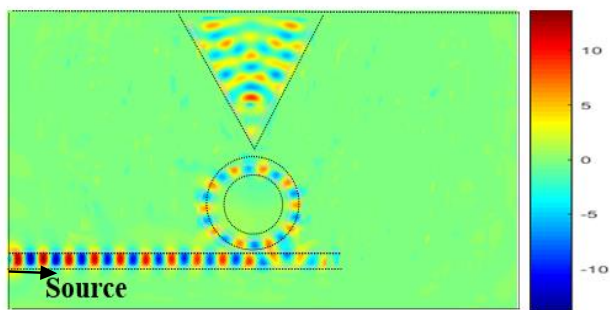


Fig. 2.  $H_x$  field pattern in the V-shaped channel for a nanowire (Au) thickness of 7 nm and  $n = 1.443$ .

changes accordingly. The  $H_x$  field pattern is illustrated in Fig.5, where it can be seen that the transmitted light is confined in the nanowire. It is worth stating that, while decreasing the  $g_2$ , the resonance becomes more considerable

due to small losses.

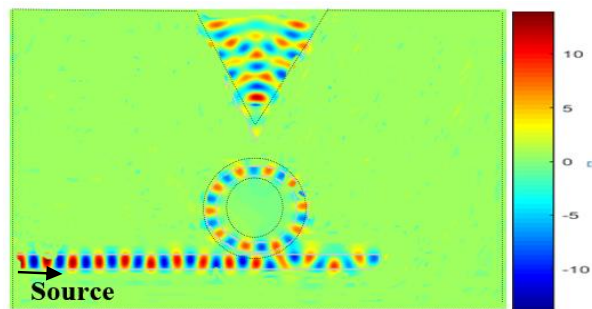


Fig. 3.  $H_x$  field pattern in the V channel for a nanowire (Au) thickness of 10 nm and  $n = 1.443$ .

Based on our simulated results illustrated in figures 3 and 4, we can see that the optical mode is highly confined in the VSC region when  $g_1 = g_2 = 31$  nm. The optical modes surrounding the nanowire can be exploited to create a coherent interaction with the biomolecules.

The observed confinement is due to the formation of the plasmon modes around the nanowire, at the resonance wavelength, where the core-guided mode couples with the SPP mode, consequently the resonance peak is excited. As a result of this, the optical modes are transmitted and propagate in the VSC sensing region. This leads to a strong light interaction with the analytes, thus a high sensitivity is achieved.

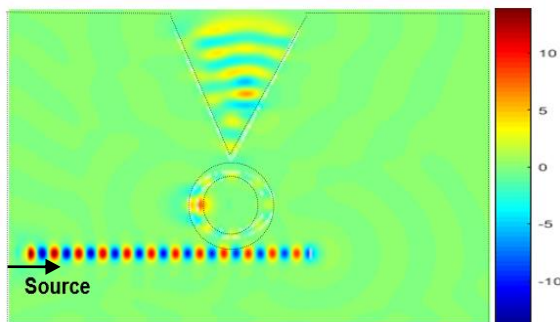


Fig. 4.  $H_x$  field pattern in the V-shaped channel for a nanowire (Au) thickness of 10 nm,  $n = 1.443$  while  $g_1 = 29$  nm and  $g_2 = 33$  nm.

In Fig. 6, the field pattern of the excited mode is illustrated, we notice that the light suffers losses and the power in the V-channel is very weak.

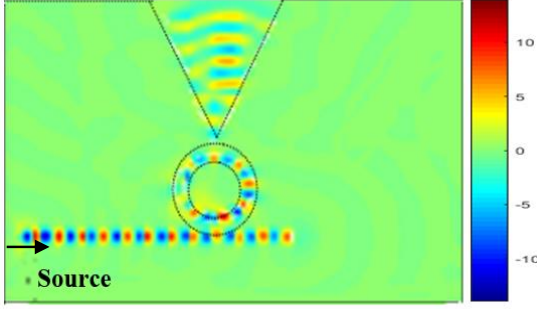


Fig. 5.  $H_x$  field pattern distribution in the V-shaped channel for a nanowire (Au) thickness of 10 nm,  $n = 1.443$  while  $g_1 = 33\text{nm}$  and  $g_2 = 29\text{nm}$ .

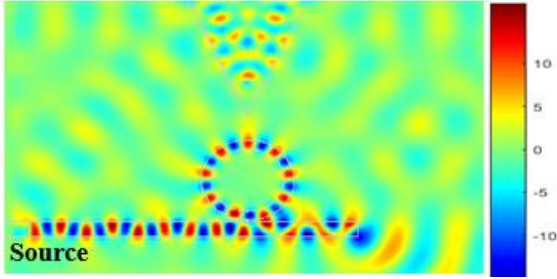


Fig. 6.  $H_x$  field pattern of the first excited mode in the V-shaped channel for a nanowire (Au) thickness of 10 nm,  $n = 1.443$  while  $g_1 = 33\text{nm}$  and  $g_2 = 29\text{nm}$ .

From figure 6 and compared to previous cases, we consider the fundamental mode through the rest of the paper.

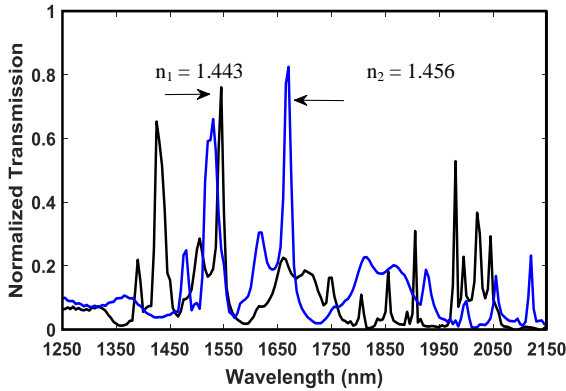


Fig. 7. Transmission spectra obtained for a nanowire (Au) thickness of 10 nm and when the V channel is filled firstly with  $n_1=1.443$  then filled with  $n_2=1.456$ . The wavelength shift is about 120 nm.

Figure 7 shows the transmission spectrum of the proposed sensor when the channel is filled with analyte (biomolecules) with refractive indices of  $n_1 = 1.443$  and  $n_2 = 1.456$ . The resonance wavelength exhibits two peaks located at  $\lambda_{\text{resonance}} = 1550\text{ nm}$  and at  $\lambda_{\text{resonance}} = 1670\text{ nm}$ , respectively. The effective index of the medium changes, leading to a shift of the resonant peak. It is convenient to define the spectral sensitivity which is related to the amount of the wavelength shift and its corresponding change in the refractive index [25]

$$S = \frac{\Delta\lambda}{\Delta n} \text{ (nm/RIU)} \quad (4)$$

Where  $\Delta\lambda$  is the wavelength variation and  $\Delta n$  represents the refractive index variation. The VSC sensing region is filled with aqueous solution containing the biomolecules with refractive index of 1.456, when the surface is poorly covered, the biomolecules are partially attracted, hence the refractive indices decreases to 1.443. In this range, the resonance wavelength shift is about 120 nm, therefore the sensitivity  $S = 9230\text{ nm/RIU}$ . It can be noticed that with 0.013 variations in the refractive index, the shift of the resonance wavelength is observed and determined. This information is necessary parameter for the fabrication of the proposed sensor. Also, the high sensitivity value of 9230 nm/RIU is an excellent property of the proposed sensor compared to their plasmonic counterparts. The quality factor is also an important device parameter for the sensing performance, it can be expressed;

$$Q = \frac{\lambda}{\Delta\lambda} \quad (5)$$

where  $\lambda$  is the central wavelength, and  $\Delta\lambda$  is the Full Width at Half Maximum (FWHM). In this proposed sensor design, the  $Q$  is evaluated to 1937. Another sensor performance parameter is also the Detection Limit ( $DL$ ), which is calculated by [26]

$$DL = \frac{\lambda}{10SQ} \quad (6)$$

where  $S$  is the sensitivity and  $Q$  stands for the quality factor. The calculated  $DL$  for the proposed sensor is  $8.5 \times 10^{-6}\text{ RIU}$ .

The Figure of Merit (FOM) is obtained by dividing the sensitivity  $S$  with the FWHM;

$$FOM = \frac{S}{\Delta\lambda_{FWHM}} \quad (7)$$

where  $\lambda$  is the resonant wavelength. The FOM for this proposed sensor is  $1.172 \times 10^4\text{ RIU}^{-1}$ .

Next, in order to evaluate the characteristics of the proposed sensor, the field intensity in the sensing region is calculated for different analyte refractive indices.

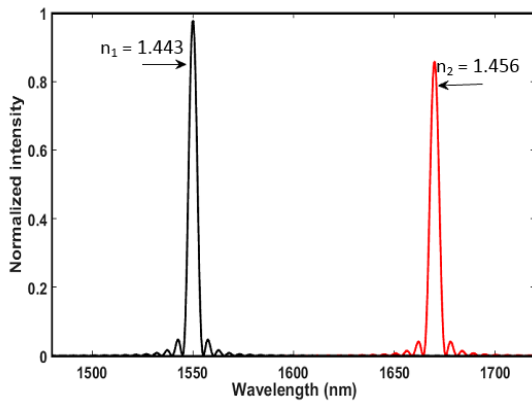


Fig. 8. Light Intensity for a nanowire (Au) thickness of 10 nm when the V-shaped channel is filled firstly with  $n_1 = 1.443$  then filled with  $n_2 = 1.456$ , the first resonance peak is located at 1550 nm, while the second one is located at 1670 nm. The wavelength shift is about 120 nm.

Figure 8 illustrates the light intensity as a function of the wavelength when  $n_1 = 1.443$  and  $n_2 = 1.456$ , respectively. The displacement of the resonance peak can be clearly observed from this figure. It can be noticed that a larger refractive index difference will lead to a larger shift of the resonance wavelength. Two resonance peaks are present in the optical spectra, the first one is located at  $\lambda_1 = 1550$  nm while the second one is positioned at  $\lambda_2 = 1670$  nm, the resonance wavelength shift is about 120 nm. This is an important feature of the proposed sensor that has not been achieved in other plasmonic resonance sensor. The observed shift is attributed to an increase in the permittivity as well as changes in the size of the resonator surface caused by the coupling of the core-guided mode and surface plasmons.

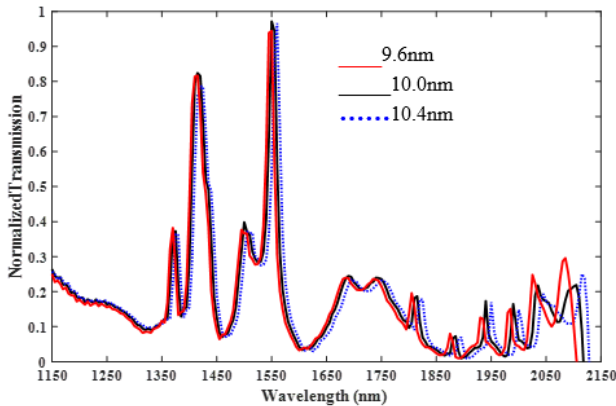


Fig. 9. Transmission spectra obtained for a nanowire (Au) thickness  $\Delta r = 9.6$  nm, 10 nm, and 10.4 nm, when the V-channel is filled with  $n_1 = 1.443$

In the proposed design, we have investigated the fabrication tolerance of  $\pm 4\%$  in the structural parameter illustrated in Fig. 9. In this figure, we have illustrated the transmission variation when  $\Delta r = 10$  nm  $\pm 0.4$  nm, and when the nanowire (Au) thickness varies for 0.4 nm ( $\Delta r = 10.4$  nm,  $\Delta r = 9.6$  nm). This figure shows that transmission varies slightly when  $\Delta r$  fluctuates between  $\pm 0.4$  nm around 10 nm. This variation in thickness is within the fabrication tolerance since the shift in transmission is very small.

After we have optimized the single V channel sensor design structure and investigated the sensor performance for different analytes, we extended the design from single V channel to double V channels. The double V channel sensor can be realized in different ways, and here we simply consider two V channels adjacent to each other to create a resonance system. The two V channels are placed side by side with spacing of  $W$ , which helps to achieve strong coupling. The schematics of the double V-shaped channels is illustrated in Fig. 10.

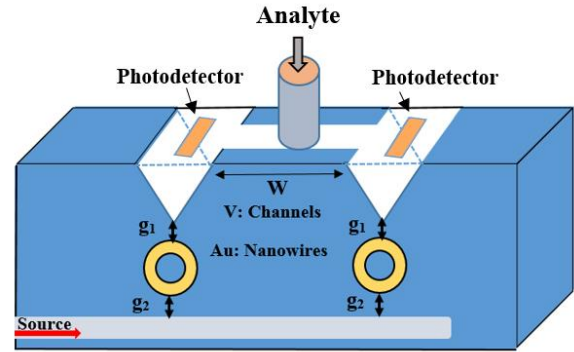


Fig. 10. Three-dimensional view of the double V-shaped channels separated by a spacing  $w$ , which are coupled to the source through the gold nanowire. The proposed sensor is able to detect various analytes simultaneously.

In order to study the effects and the influence of the second V channel and the amount of light transferred to the second V channel, we keep the gaps  $g_1$  and  $g_2$  and  $n_1 = 1.443$ ,  $n_2 = 1.456$  fixed while the spacing  $W$  is varied; 465 nm, 155 nm and 620 nm. In Fig. 11, we illustrate the  $H_x$  field pattern distribution inside the coupled V channels when  $W = 465$  nm, where it can be clearly seen that the  $H_x$  field is well confined. The coupling of the guided mode with the SPP mode results in strong confinement of the field intensity, therefore the proposed sensor is very sensitive to the slight changes in the refractive index. The FDTD simulations are performed initially for outer radius = 589 nm and inner radius = 465 nm, then we vary the thickness  $\Delta r$ , which is defined as  $\Delta r = \text{outer radius} - \text{inner radius}$ , ( $\Delta r = r_{\text{out}} - r_{\text{in}}$ ).

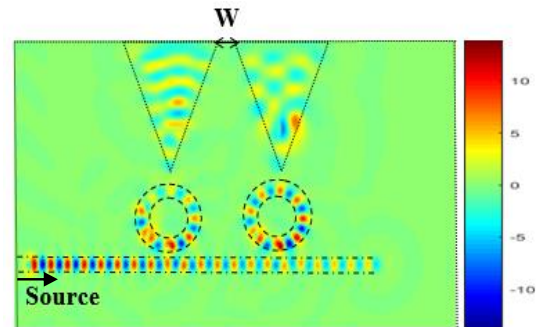


Fig. 11.  $H_x$  field pattern distribution in the coupled V-shaped channels for a nanowire (Au) thickness of 10 nm, When the left V channel is filled with  $n_1 = 1.443$ , and the second one is filled with  $n_2 = 1.456$  while  $g_1 = g_2 = 31$  nm for a spacing  $W = 465$  nm.

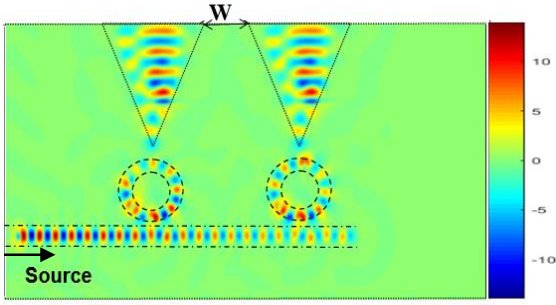


Fig. 12.  $H_x$  field pattern distribution for a nanowire (Au) thickness of 10 nm, when the left and the right V channels are filled with  $n_1=1.443$ ,  $n_2=1.456$ , respectively, while  $g_1 = g_2 = 31\text{nm}$  when  $W = 155\text{nm}$ .

Figure 12 shows the snapshot of the  $H_x$  field pattern distribution when  $W = 155\text{ nm}$ , we notice that the light suffers losses as it propagates towards the second V channel. To investigate the effect of the spacing between the V channels, we have increased  $W$  from 155nm to 620nm, the corresponding  $H_x$  field pattern evolution is depicted in Fig. 13. It can be observed that the light intensity disappears, therefore the sensor is not sensitive to the changes of the surrounding environment.

Comparing the  $H_x$  field pattern distribution in figures 11, 12 and 13, it can be clearly seen that the strongest coupling is achieved when  $W$  is 465 nm. To optimize the performances of the sensor under different analytes, the spacing  $W$  is kept fix to 465 nm, we then calculate the transmission spectra when the left V channel is filled with analyte refractive index 1.443 and the right V channel with 1.456. The transmission spectra when two different analytes are investigated simultaneously are illustrated in Fig. 14. From this figure, one can see that the resonant wavelength peaks are centered at  $\lambda_1 = 1550\text{ nm}$  and  $\lambda_2 = 1750\text{ nm}$ , respectively. The sensitivity is calculated, using equation (4), to be 15384 nm/RIU. This result is increased significantly compared with the sensitivity for a single VSC and it is enhanced by 6154 nm/RIU. The sensitivity reported in literature [7] is about 4471 nm/RIU, while our design predicts a sensitivity of about 15384 nm/RIU. Also, the sensor resolution is determined to be as good as  $5.2 \times 10^{-6}$  RIU.

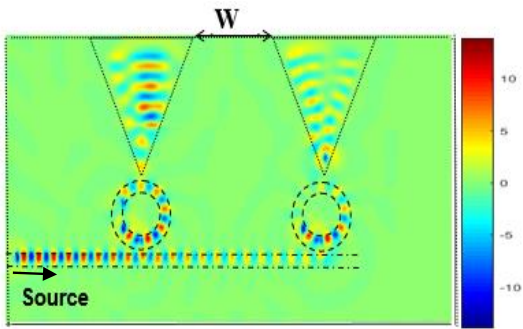


Fig. 13.  $H_x$  field pattern evolution in coupled V-channels for a nanowire (Au) thickness of 10 nm, When the left V channel is field with  $n_1=1.443$ , and the right one with  $n_2=1.456$  and  $g_1 = g_2 = 31\text{nm}$  when  $W = 620\text{ nm}$ .

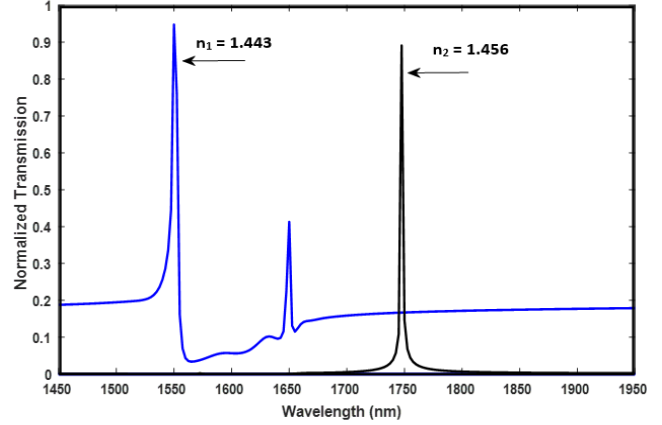


Fig. 14. Transmission spectra for a nanowire (Au) thickness of 10 nm when the left and right V-shaped channels are filled with  $n_1=1.443$  and  $n_2=1.456$ , respectively, the double channels are separated by a distance  $w= 465\text{nm}$ . The left resonance wavelength is located at 1550 nm and the right one is centred at 1750 nm. The wavelength shift is about 200 nm.

The double VSC sensor has an excellent sensitivity nearly 1.6 times higher than that obtained for the single VSC. This clearly indicates that our dual channel V-shaped sensor exhibits very high sensitivity and selectivity.

#### IV. FABRICATION

The proposed V-shaped channel mediated gold nanowire sensor can be fabricated using standard micro fabrication techniques such as electron beam lithography, inductively coupled Reactive ion etching, and glancing angle evaporation methods. The waveguide is composed of a 50 nm thick silica deposited by low pressure Chemical Vapor Deposition (LPCVD) on bulk silicon. In order to operate in a single mode, the waveguides are defined either by e-beam or Deep Ultra Violet (DUV) lithography. Above the waveguide, a local etching is performed to remove the middle section then a gold nanowire is deposited on the etched region. The pattern consisting of an array of holes would be defined using electron-beam lithography according to the above layout. The V-shape can be performed by inductive coupled reactive ion etching using CHF3 and BCl3 dry etch chemistry and a durable resist mask (ZEP). The inductive coupled plasma process conditions can be adjusted to provide straight vertical side walls through the volume of the core layer (aspect ratios of 4:1 are easily achievable). With the remaining resist mask of 4:1 are easily achievable). With the remaining resist mask in place, the structure would then be coated with a thin gold layer by glancing angle e-gun evaporation. On top of the V-shape channel a flow container is attached with two connections to provide an inlet (analytes) and outlet.

To couple light into the device grating couplers, would be etched into the PLC to couple light into the device from the top. Scanning Near field Optical Microscopy (SNOM) would be used to test operation of the device. The output transmission is recorded using a photodetector and a digital oscilloscope placed at the end of the channel.

## V. CONCLUSION

This paper demonstrates a unique and highly sensitive proposal based on refractive index sensors on single and double V-Shaped Channel (VSC) coupled with Au-nanowire. The transmission characteristics and the light intensity for different refractive indices have been investigated. It is found that the resonance wavelength shifts about 120 nm for the single VSC, while this shift has been increased enormously to reach 200 nm for double shaped channel. In comparison to single VSC, the double VSC presents superior performances in terms of sensitivity and sensor resolution. We believe that the proposed sensor design has great potential to be implemented in lab on a chip platform to detect the origin of infection diseases. The proposed Proof of concept (PoC) photonic sensor would have great impact on designing high sensitive and selective multichannel next generation biophotonics methods and devices, as research tools, to understand the cellular origin of infectious disease.

## ACKNOWLEDGMENT

This project was funded by the Deanship of Scientific Research (DSR), King Abdulaziz University, Jeddah, under grant No. (D-294-305-1441). The authors, therefore, gratefully acknowledge the DSR technical and financial support.

## REFERENCES

- [1] V. E. Bochenkov, M. Frederikson, D.S. “Elevated Sutherland, Enhanced refractive index sensitivity of short-range ordered nanohole arrays in optically thin Au plasmonic films,” *Opt. Express* 21, 14763, 2013.
- [2] R. Verma, S.K. Srisvastava, B.D. Gupta, “Surface-plasmon-resonance based fiber-optic sensor for the detection of low density of lipoprotein,” *IEEE Sens.J.* 12, 3460, 2012.
- [3] J. He, S. Yang, “Line shapes in a plasmonic waveguide system based on plasmon-induced transparency and its application in nanosensor,” *Opt.Commun.* 381, 163, 2016.
- [4] D.K. Gramotnev, S. I. Bozhevolnyi, “Plasmonics Beyond the diffraction limit,” *Nat. Photonics* 4, 83, 2010.
- [5] M. Saifur Rahman, Md. Shamim Anower, L. F. Abdulrazak “Modeling of a fiber optic SPR biosensor employing Tin Selenide (SnSe) allotropes,” *Results in Physics*, 15, 1026232, 2019.
- [6] A. Dolatabady, N. Granpayeh, V. F. Nazhad, “A nanoscale refractive index sensor in two dimensional plasmonic waveguide with nanodisk resonator,” *Opt.Commun.* 300, 265, 2013.
- [7] A. K. Pathak, B.M.A.Rahman, K. Singh and S. Kumari, Sensitivity Enhancement of a Concave Shaped Optical Fiber Refractive Index Sensor Covered with Multiple Au Nanowires, *Sensors*,19, 4210, 2019
- [8] M.K. Hossain, M.T. Rahman, M.K. Basher, M.J. Afzal, M.S. Basher, Impact of ionization radiation doses on nanocrystalline TiO<sub>2</sub> layer in DSSC's photoanode film, *Results in Physics* 11, 1172, 2018
- [9] I. Abdelaziz, F. AbdelMalek, S. Haxha, H. Ademgil, H. Bouchriha, “Photonic Crystal Fiber with Ultrahigh Birefringence and Flattened Dispersion by Using Genetic Algorithms,” *Journal of Lightwave Technology*, Jan. 15, *IEEE, JLT*,31, 343, 2013.
- [10] T. Wu, Y. Liu, Z. Yu, Y. Peng, C. Shu, H. Ye, “The sensing characteristics of plasmonic waveguide with a ring resonator,” *Opt. Express*. 22, 7669, 2014.
- [11] M. R. Rakhshani, M. A. Mansouri-Birjandi, “Utilizing the metallic nano rods in hexagonal configuration to enhance sensitivity of plasmonic racetrack in resonator applications,” *Plasmonics* 2016.
- [12] M. Li, S. K. Cushing, N. Wu, “Plasmon- enhanced optical sensor,” a review, *Analyst* 140, 386, 2015.
- [13] Y. Ishizaka, S. Makino, T. Fujisawa, and K. Saitoh, “A metal-assisted silicon slot waveguide for highly sensitive gas detection,” *IEEE Photon. J.*, vol. 9, no.1, Feb., Art. no. 6800609, 2017.
- [14] L. Zhou, X. Sun, X. Li, and J. Chen, “Miniature microring resonator sensor based on a hybrid plasmonic waveguide,” *Sensors*, 11, 7, 6856, 2011.
- [15] M. S. Kwon, “Theoretical investigation of an interferometer-type plasmonic biosensor using a metal-insulator-silicon waveguide, *Plasmonics*,” 5, 4, 347, 2010.
- [16] J. Nyagilo, S. H. Chang, J. Wu, Y. Hao, D. P. Dave. “Fiber-tip plasmonic resonators for label-free biosensing,” *Sens. Actuators B* 212, 225, 2015.
- [17] B. Liu, Y. Lu, X. Yang, J. Yao, “Tunable Surface Plasmon Resonance Sensor Based on Photonic Crystal Fiber Filled with Gold Nanoshells,” *Plasmonics*, 13, 763, 2018.
- [18] J. G. Yun, J. Kim, K. Lee, Y. Lee, and B. Lee, “Numerical study on refractive index sensor based on hybrid-plasmonic mode,” *Proc. SPIE*, 10323, Art. no. 103236U, 2017.
- [19] R. Otupiri, E.K. Akowuah, S. Haxha, “Multi-channel SPR biosensor based on PCF for multi-analyte sensing applications,” *Opt Express* 23, 15716, 2015.
- [20] A. K. Pathak, V. K. Singh, S. Ghosh, and B. M. A. Rahamn, Investigation of a SPR based refractive index sensor using a single mode fiber with a large D-shaped microfluidic channel, *OSA, Continuum*, vol.2, N.11, 3009, 2019.
- [21] Q. Li and M. Qiu, “Plasmonic wave propagation in silver nanowires: guiding modes or not?,” *Opt. Express*, 21, 7, 8587, 2013.
- [22] A. Taflove, S. G. Johnson, A. Oskooi, “Advances in FDTD Computational Electrodynamics: Photonics and Nanotechnology (Artech House Antennas and propagation Library) Unabridged, 28 Feb 2013.
- [23] D. Shelton “Optical properties of metallic films,” *Plasmonics Inc., USA*, 547-589, 2014.
- [24] J. Zhang, L. Zhang and W. Xu, “Surface plasmon polaritons: physics and applications,” *J. Phys. D: Appl. Phys.* 45, 113001, 2012.
- [25] C. Ciminelli, F. Dell’Olio D. Conteduca, C. M. Campanella M.N. Armenise “High performance SOI microring resonator for biochemical sensing,” *Optics & Laser Technology*, 59, 60-67, 2014.
- [26] S. Arafa, M. Bouchemata, T. Bouchemata, A. Benmerkhi, A. Hocini, “Infiltrated photonic crystal cavity as a highly sensitive platform for glucose concentration detection,” *Opt. Commun.* 384, 93, 2017.